Arch. Mech., 41, 6, pp. 821–835, Warszawa 1989

Doppler signal predictions using the Lorenz–Mie theory for applications to measurements in two-phase flows

A. CENEDESE, F. CIOFFI and G. P. ROMANO (ROMA)

IN RECENT YEARS many systems based on Laser Doppler Anemometry for the simultaneous measurements of velocity, dimensions and concentration of particles dispersed in a fluid have been proposed. Theoretical aspects of the light diffusion phenomena in the analysis of particle dimensions and concentrations have still to be solved. For this reason the theoretical predictions of the behaviour of the light diffused field produced by particles crossing the light beams seem to be necessary. In this work the light scattered from a particle crossing two Laser beams focalized in a common measuring volume using Mie optics is examined. For different particle trajectories and a given set-up of the transmitting and collection optics, the characteristics of the Doppler signal — amplitude, phase and modulation — have been investigated.

W ostatnich latach zaproponowano wiele układów opartych na anemometrii dopplerowskiej i służących do jednoczesnego pomiaru prędkości, rozmiarów i koncentracji cząsteczek rozproszonych w płynie. Wymagają dalszego wyjaśnienia pewne aspekty teoretyczne dotyczące dyfuzji światła w analizie rozmiarów i koncentracji cząsteczek. W tym celu wydaje się konieczne przeanalizowanie teorii pola rozproszenia światła wywołanego przecinaniem promieni świetlnych przez tory cząsteczek. W pracy przeanalizowano problem rozproszenia na cząsteczce dwóch promieni laserowych skupionych w jednej objętości pomiarowej. Zbadano charakterystyki amplitudy, modulacji i fazy sygnału dopplerowskiego przy różnych trajektoriach cząsteczek w przyjętym układzie optycznym typu Mie.

В последних годах предложено много систем, опирающихся на доплеровской анемометрии и служащих для одновременного измерения скоростей, размеров и концентрации частиц рассеянных в жидкости. Требуют дальнейшего выяснения некоторые теоретические аспекты, касающиеся диффузии света в анализе размеров и концентрации частиц. С этой целью кажется необходимо проанализировать теории поля рассеяного света, вызванного пересечением световых лучей через траектории частиц. В работе проанализирована задача рассеяния на частице двух лазерных лучей, сосредоточенных в одном измерительном обдеме. Исследованы характеристики амплитуды, модуляции и фазы доплеровского сигнала при разных траекториях частиц в принятой оптической системе Ми.

1. Introduction

TWO-PHASE FLOWS in which a particular phase is dispersed in a fluid phase are encountered in many fields of engineering. Characterization of those flows requires the accurate measurement of the particle distribution, simultaneous size and velocity measurements of individual particles, trajectory for each size class, particle number density and volume flux. The optical methods based on Laser Doppler Anemometry (LDA), which have had a rapid development during the last decade, seems to be particularly suitable to obtain the informations listed above [1]. These methods have the advantage of allowing measurements without disturbing the flow field and have the same spatial and temporal resolution of LDA, successfully used in monophase flows.

The methods are based on light scattering from particles dispersed in the fluid and crossing a measurement volume which is defined by two or more intersecting laser beams;

http://rcin.org.pl

the size and the velocity of the particles have to be correlated by monotonous relationships to a measurable quantity of the diffused light field: frequency, amplitude, modulation and phase of the Doppler signal [2, 3, 4, 5]. While few problems arise for the velocity measurements, a lot of problems have to be resolved for size measurements. The scattering of light is in fact a very complicated process, highly conditioned by both optical and geometrical characteristics of the particles and of the transmitting and collection optics; so it is not easy to find a relationship valid for all situations. For these reasons theoretical predictions about the behaviour of the scattered light, for given particle characteristics and optical configuration, are needed.

In the paper some preliminary results obtained by a three-dimensional Lorentz–Mie calculation program are presented; the program is capable of simulating the scattered light from a spherical particle crossing the measuring volume defined by two intersecting Gaussian laser beams. Amplitude, phase and modulation of the Doppler signal for different optical configurations and different particle sizes are examined. Furthermore the problems associated with the particle trajectory in the measuring volume are stressed.

2. Light scattering from spherical paerticles

An exact solution for the scattering of electromagnetic waves by a spherical dielectric body was first obtained by MIE [6]. In recent years the theory has been generalized for arbitrary particle dimensions [7, 8] and many efforts to remove the hypothesis of sphericity and of plane incident wave are being made [9, 10].

An easier approach is obtained by using geometrical optics, but reflection, refraction and diffraction are not always separable and in general situations it is more rigorous to solve Maxwell' s equations with proper boundary conditions.

Following Mie, we will describe the incident beam as a monochromatic, linearly polarized, electromagnetic plane wave diffused by a spherical, homogeneous and isotropic particle; the intensity Gaussian profile of the incident beam is simulated by the sum of plane profiles on the particle surface. The particle-beam interactions produce amplitude, phase and polarization variations of the scattered light field. The boundary conditions on the particle surface result from the continuity of the electric and magnetic field tangential components.

For distances of observation, R, much larger than the wavelength λ, the intensity of the diffused light will depend only on the parameter $q = \pi d/\lambda$ (d is the particle diameter), on the physical properties of the medium and it will change with the scattering angle θ between the incident and observation directions.

The diffused electric field will be completely described by the parallel and perpendicular components to the scattering plane, i.e., the one defined with the incident and scattering directions [7]:

$$
\begin{aligned}
E_{||} &= \mathrm{Re}(|A_{||}(\theta, \Phi, R)|e^{i(\Omega t + \Delta\varphi_{||})}), \\
E_{\perp} &= \mathrm{Re}(|A_{\perp}(\theta, \Phi, R)|e^{i(\Omega t + \Delta\varphi_{\perp})}),
\end{aligned}
\tag{2.1}
$$

where Re indicates the real part, $A_{||}(\theta, \Phi, R) = A^0|S_{||}(\theta)| \cos\Phi/(K R)$; $A_{\perp}(\theta, \Phi, R) = A^0|S_{\perp}(\theta)|\mathrm{sen}\Phi/(KR)$; A^0 is the initial amplitude; $K = 2\pi/\lambda$; θ, Φ, R is a polar coordinate system centered on the particle (Fig. 1), $\Omega = 2\pi c/\lambda$.

http://rcin.org.pl

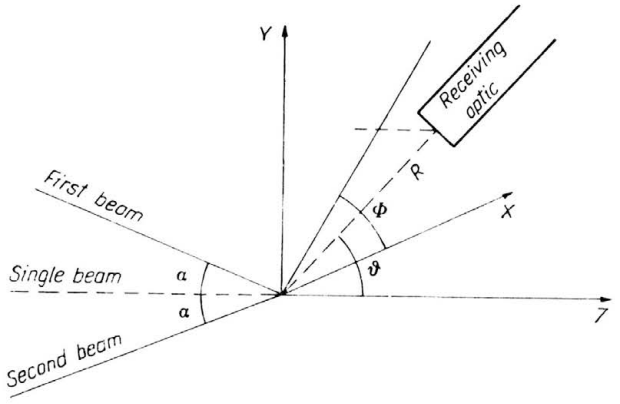

FIG. 1. Coordinate system for 1-beam, 2-beams case.

$S_\perp$ and $S_{||}$ are the well-known scattering functions expressed in terms of the parameter q and of the real and imaginary part of the refractive index through the Riccati–Bessel and Legendre functions: therefore it is possible to use recurrence relationships to evaluate numerically the scattering functions [11]. The terms $\Delta\psi_{||}$ and $\Delta\psi_\perp$ are responsible for the different phases of the two electric fields. We can write it as the sum of three terms:

$$\begin{aligned} \Delta\psi_{||} &= \varphi(t)+2\pi R(t)/\lambda+\Gamma_{||}(\theta), \\ \Delta\psi_\perp &= \varphi(t)+2\pi R(t)/\lambda+\Gamma_\perp(\theta), \end{aligned} \tag{2.2}$$

where:

$\varphi(t)$ is the phase shift for the movement with respect to the incident wave which is given by [11]:

$$\varphi(t) = \varphi^0 - 2\pi(\mathbf{v}\cdot\mathbf{i})t/\lambda$$

in which $\mathbf{v}$ is the particle velocity, φ^0 is the initial phase and $\mathbf{i}$ is the unit vector in the incident direction;

$R(t)$ is the phase shift for the motion with respect to the receiver:

$$R(t) = R^0 - (\mathbf{v}\cdot\mathbf{r})t$$

in which $\mathbf{r}$ is the receiving direction unit versor;

$\Gamma_{||}(\theta)$ and $\Gamma_\perp(\theta)$ are the phase shift of the two different electric fields due to the receiver position and particle characteristics:

$$\Gamma_{||}(\theta) = \operatorname{arctg}[\operatorname{Im}(S_{||})/\operatorname{Re}(S_{||})],$$

$$\Gamma_\perp(\theta) = \operatorname{arctg}[\operatorname{Im}(S_\perp)/\operatorname{Re}(S_\perp)]$$

in which Im indicates the imaginary part.

The first two terms in Eqs. (2.2) which are responsible for the Doppler shift are dependent on the velocity and then on the time; for a distance of observation much larger than the typical measurement volume dimension, the third term is dependent only on the scat-

http://rcin.org.pl

tering direction and on the particle characteristics (size, shape, refractive index). Small deviations from the spherical shape will produce strong variations in the light intensity distribution [11].

If more particles or beams are present, the scattered light fields, independently produced by each particle or beam, interfere in relation to their relative phases.

The case of two incident beams on a particle moving along an arbitrary trajectory in the measurement volume has been investigated. The scattered light is collected with a receiver situated in an arbitrary position, with arbitrary shape and dimensions.

A calculation program for the computation of the scattered light field amplitude, phase and polarization has been developed for this general situation, starting from a single beam with stationary particles and a point-like detector calculation program [12]. The four electric fields $E_{\|1}$, $E_{\|2}$, $E_{\perp 1}$, $E_{\perp 2}$ have to be decomposed in their components in an orthogonal three-axis system (Fig. 1):

$E_{\|1}$, $E_{\perp 1}$ indicate the parallel and perpendicular components to the scattering plane 1 containing the incident beam 1 and the observation directions;

$E_{\|2}$, $E_{\perp 2}$ are the same for the incident beam 2.

In Appendix A the directions of the four electric fields and the components along the x, y, z-axis are calculated.

From Eq. (2.1) we can write for the electric fields modulus

$$
\begin{aligned}
|E_{\|1}| &= \mathrm{Re}(|A_{\|1}(\theta, \Phi, R)|e^{i(\Omega_1 t + \Delta\psi_{\|1})}),\\
|E_{\perp 1}| &= \mathrm{Re}(|A_{\perp 1}(\theta, \Phi, R)|e^{i(\Omega_1 t + \Delta\psi_{\perp 1})}),\\
|E_{\|2}| &= \mathrm{Re}(|A_{\|2}(\theta, \Phi, R)|e^{i(\Omega_2 t + \Delta\psi_{\|2})}),\\
|E_{\perp 2}| &= \mathrm{Re}(|A_{\perp 2}(\theta, \Phi, R)|e^{i(\Omega_2 t + \Delta\psi_{\perp 2})}),
\end{aligned}
\tag{2.3}
$$

where Ω_1 and Ω_2 are the frequencies of the two beams, the quantities A are calculated in the same way of Eqs. (2.1) and the terms $\Delta\psi_{\|}$ and $\Delta\psi_{\perp}$ are expressed like in Eqs. (2.2), where the quantity R is the same for the two beams, while the quantities λ, $\Gamma_{\|}$, $\Gamma_{\perp}$ and φ are different.

The final intensity on the receiver will be

$$I = \overline{E_x^2} + \overline{E_y^2} + \overline{E_z^2}$$

with

$$\overline{E_x^2} = \frac{1}{T}\int_0^T (E_{\|x1} + E_{\|x2} + E_{\perp x1} + E_{\perp x2})^2\, dt, \tag{2.4}$$

where T is the integration time of the photoreceiver. Since $T \approx 10^{-7}$ s is much larger than $1/\Omega_1 \approx 1/\Omega_2 \approx 10^{-15}$ s, the terms containing the frequencies Ω_1, Ω_2 and multiples give no contributions. The same is for y and z components.

The final expression of the intensity contains the phase differences between the electric field components that modulate the interference terms

$$
\begin{aligned}
I = {} & A(\theta, \Phi, R) + B(\theta, \Phi, R)\cos[(\Omega_1 - \Omega_2)t + (\Delta\psi_{\|1} - \Delta\psi_{\|2})]\\
& + C(\theta, \Phi, R)\cos[(\Omega_1 - \Omega_2)t + (\Delta\psi_{\|1} - \Delta\psi_{\perp 2})] + D(\theta, \Phi, R)\cos[(\Omega_1 - \Omega_2)t\\
& + (\Delta\psi_{\perp 1} - \Delta\psi_{\|2})] + E(\theta, \Phi, R)\cos[(\Omega_1 - \Omega_2)t + (\Delta\psi_{\perp 1} - \Delta\psi_{\perp 2})]
\end{aligned}
\tag{2.5}
$$

http://rcin.org.pl

in which A, B, C, D, E are functions of $A_{\|1}, A_{\|2}, A_{\perp 1}, A_{\perp 2}$ (complete expressions are given in Appendix A). For a given scattering direction, there are different amplitudes and phases in the scattered light fields.

The angles θ and Φ for the two beams are not the same as the one defined in Eqs. (2.1) and in Fig. 1; to keep a coordinate system connected to the incident beam, the angles have to be recalculated for each position (θ, Φ) of the receiver. Useful expressions are presented in Appendix B.

The calculation program gives the intensity and phase of the diffused light for particular directions of scattering, when a particle of given dimension and refractive index crosses the measurement volume with an arbitrary spatial trajectory. The dimension and shape of the receiver have also to be specified.

The calculations have been verified in the particular situation of the receiver in the same plane of the two incident beams. In this situation there is a single scattering plane: the two components perpendicular to the scattering plane from the two different beams have the same direction and so far for the parallel ones. In Eq. (2.5) the terms consisting of the interference between parallel and perpendicular components are not present: the quantities C and D are identically zero. The final expression contains the sum between the parallel and perpendicular components and only two interference terms; it is equal to the one obtained with a direct calculation by other authors [11]:

$$\begin{aligned} I = {} & A(\theta, \Phi, R) + B(\theta, \Phi, R)\cos[(\Omega_1 - \Omega_2)t + (\Delta\psi_{\|1} - \Delta\psi_{\|2})] \\ & + E(\theta, \Phi, R)\cos[(\Omega_1 - \Omega_2)t + (\Delta\psi_{\perp 1} - \Delta\psi_{\perp 2})] \\ = {} & A_{\|1}^2/2 + A_{\perp 1}^2/2 + A_{\|2}^2/2 + A_{\perp 2}^2/2 + A_{\|1}A_{\|2}\cos[(\Omega_1 - \Omega_2)t + (\Delta\psi_{\|1} - \Delta\psi_{\|2})] \\ & + A_{\perp 1}A_{\perp 2}\cos[(\Omega_1 - \Omega_2)t + (\Delta\psi_{\perp 1} - \Delta\psi_{\perp 2})]. \end{aligned}$$

3. Preliminary results

The purpose of the tests performed was to verify the reliability of the program to describe the light diffusion phenomena by spherical particles, which present a specific interest in two-phase flows. Thus the tests were related to:

Doppler signals for different trajectories in the measurement volume;

Doppler signals for a point-shaped and a rectangular collection aperture of the receiver;

phase difference between two Doppler signals in relation to the particle size and the collection optics position and dimensions;

amplitude of Doppler signals in relation to particle size and collection optics position and dimensions;

visibility of Doppler signals for different particle dimensions with different collection optics and different angle between the beams.

In the tests transparent particles (refractive index $m = 1.5$) with dimensions between 0.5 μm and 30 μm were considered. The medium refractive index has been assumed to be equal to 1.

The transmitting and collection optics have the following characteristics:

wavelength of the light equal to 0.5 μm;

observation distance equal to 70 cm (except for the visibility test 25 cm).

http://rcin.org.pl

The angle between the beams, the beams dimensions and the scattering angles are shown in each figure.

In our situation the use of the Lorenz–Mie theory instead of the simpler geometrical optics is appropriate. In fact, as explained in [7, 13, 14], three main regions can be defined in relation to the parameter $a = 2\pi dm/\lambda$ in which the use of a particular light diffusion theory is more suitable:

Rayleigh scattering	$a \leqslant 1$,
Mie optics	$1 < a < 500$,
Geometrical optics	$a \geqslant 500$.

For the optical and geometrical characteristics of the particles used in the computations, the values of the parameter a are limited between 9 and 560.

Moreover, also it has been demonstrated that in general situations the use of geometrical optics gives good approximations of the true results obtained with Mie optics [15], in particular situations when the scattering angles or the particle dimensions are such that the two results are not in good agreement [16].

In the first test different trajectories in the measurement volume were considered: in Fig. 2 three Doppler signals produced by a particle for a point-shaped collection aperture are shown; the different trajectories considered are indicated in Fig. 3. The particle velocity component normal to the fringes is the same for all the calculations.

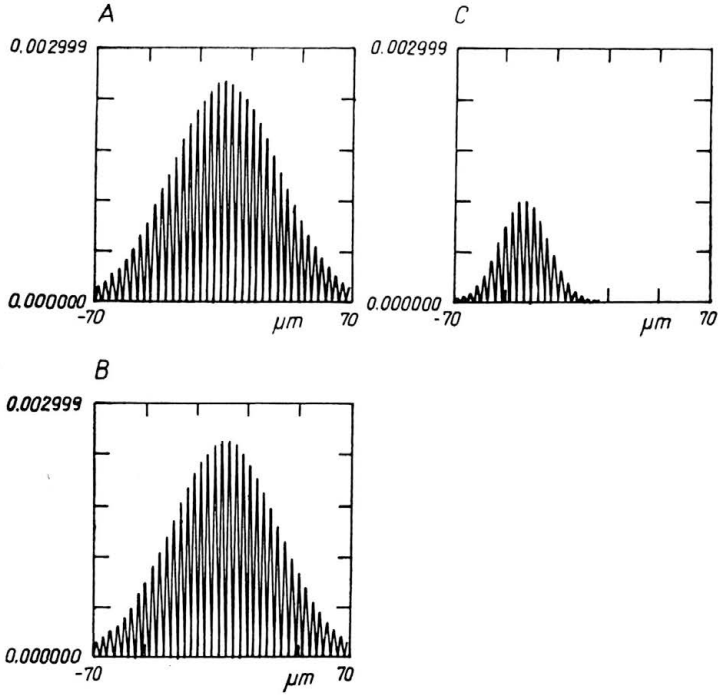

FIG. 2. Doppler signal intensity vs y-position in the measuring volume for different trajectories with a point-like receiver. Beams angle — 7.5°, beams dimension — 30 μm, particle dimension — 5 μm, scattering angles — 10°, 10°, receiver: point-like.

http://rcin.org.pl

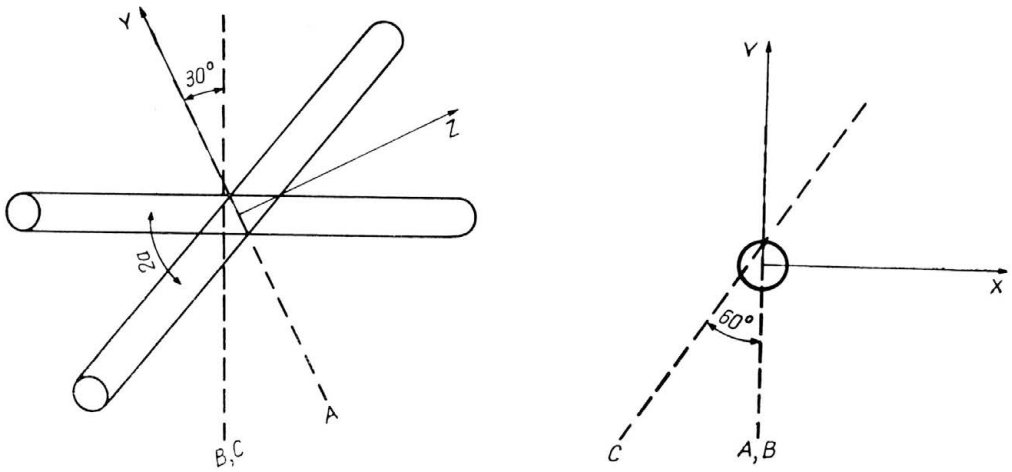

FIG. 3. Different tested trajectories in the measuring volume.

The same trajectories for a square (5 × 5) cm receiver are shown in Fig. 4: the effect of a finite collection aperture increase the pedestal due to the spatial integration over the receiver aperture. However, the differences between the signals along different trajectories still remain the same between the two situations. The intensity scales are of course different taking into account the integration of the diffused intensity over the collection aperture.

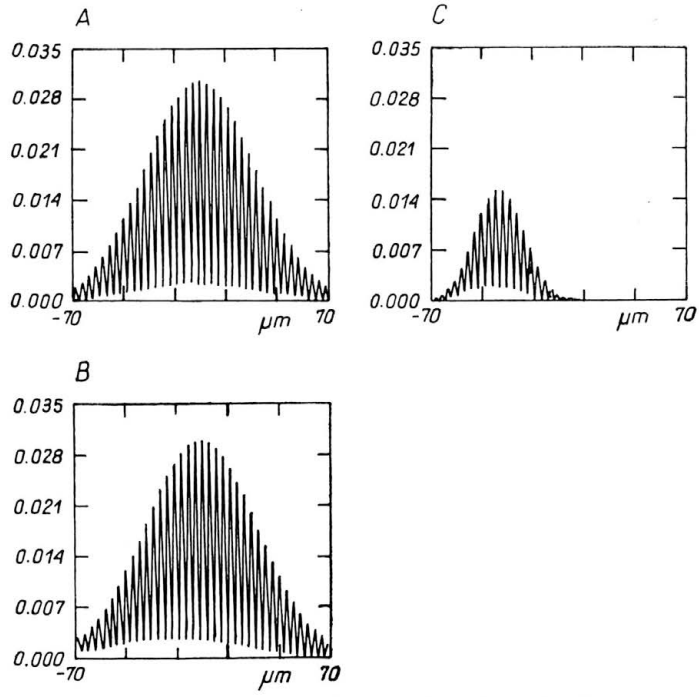

FIG. 4. Doppler signal intensity vs y-position for different trajectories with a finite receiver. Beams angle — 7.5°, beams dimension — 30 μm, particle dimension — 5 μm, scattering angles — 10°, 10°, receiver: square 5 × 5 cm.

http://rcin.org.pl

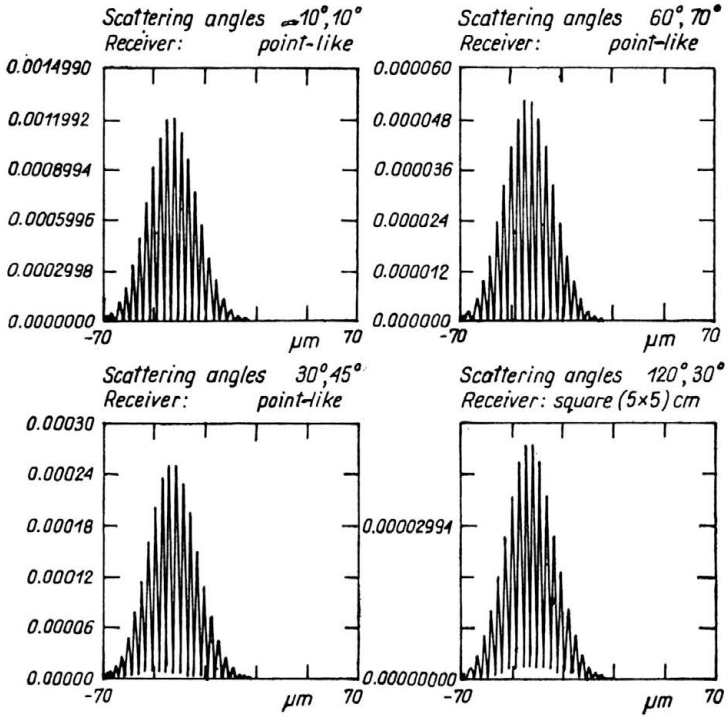

FIG. 5. Doppler signal intensity vs y-position for the C trajectory with different receivers at different scattering angles. Beams angle — 7.5°, beams dimension — 30 μm, particle dimension — 5 μm.

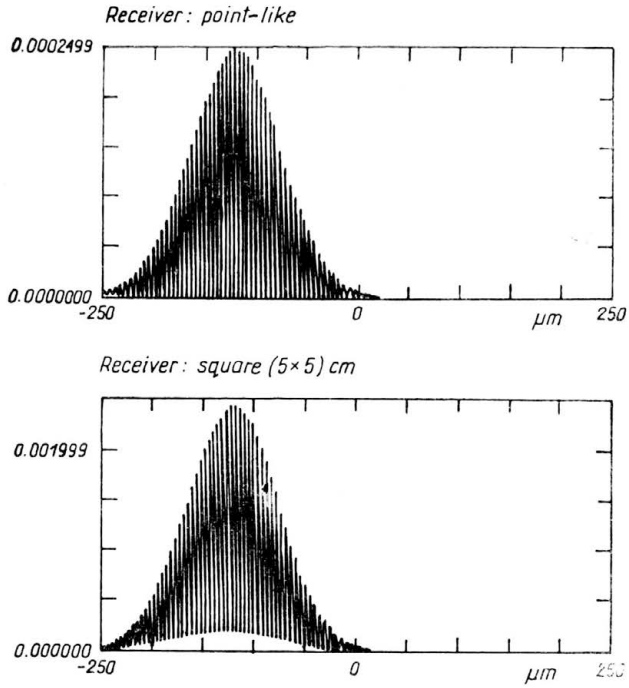

FIG. 6. Doppler signal intensity vs y-position for the C trajectory with different receivers for a 20 μm particle, Beams angle — 7.5°, beams dimension — 100 μm, particle dimension — 20 μm, scattering angles — 10°.

http://rcin.org.pl

In Fig. 5 four signals with different scattering angles and receivers for the *C* trajectory of Fig. 3 are shown: intensity and phase variations, due to the different receivers positions and dimensions, are present in the high frequency component. Instead the behaviour of the low frequency component appears invariant: the maximum position and the signal shape are the same for all situations.

The last trajectory test is concerned with a different particle diameter: 20 μm particles instead 5 μm have been used (Fig. 6). The pedestal, in the finite aperture situation, is now particularly evident. The maximum position and the shape of the low intensity component are the same as in the previous tests. It seems to be possible to individualize the trajectory of a particle in the measuring volume from the Doppler signal intensity using a low pass filter that eliminates the high frequencies: these components present phase and intensity variations for different receivers positions and particle diameter.

In the second test the phase difference between two Doppler signals detected by two receivers situated in different positions has been examined. It is known that for particular scattering angles a precise linear relationship between the phase difference and the particle diameter exists [4, 5]. In Fig. 7 the phase differences as a function of the particle diameter for an increasing receiver aperture at scattering angles (30°, 4°) and (30°, −4°) are shown. The oscillations around the linear trend are due to intensity variations in space that give rise to a characteristic lobe configuration: the number of those lobes is as great as the

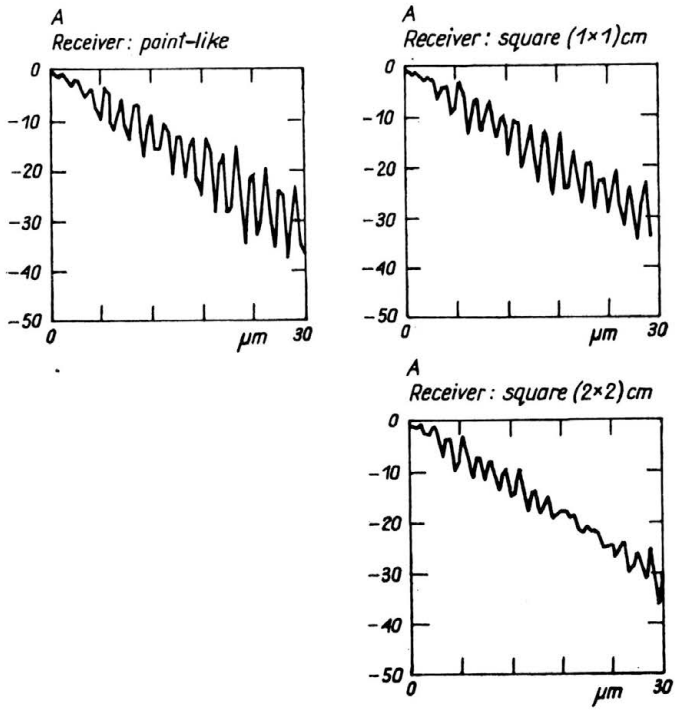

FIG. 7. Phase difference between two Doppler signals vs particle diameter for different receivers apertures at scattering angles 30°, ±4°. Beams angle — 4°, beams dimension — 300 μm, scattering angles — {30°, 4°; 30°, −4°}.

http://rcin.org.pl

particle diameter is large with respect to the receiver aperture. In fact, for an increasing receiver aperture the oscillations are averaged out especially for the bigger particles [5]. In this direction the use of particularly shaped detectors seems to be useful [15].

In Fig. 8. the same previous situations but with (70°, 4°) and (70°, −4°) scattering angles are shown. Also here for increasing receiver aperture the oscillations are averaged out, but a less defined relationship between the phase difference and the particle diameter is recognizable. For a given ratio of the particle to the medium refractive index and laser wavelength, it is necessary to individualize the best scattering angles to obtain a linear relationship.

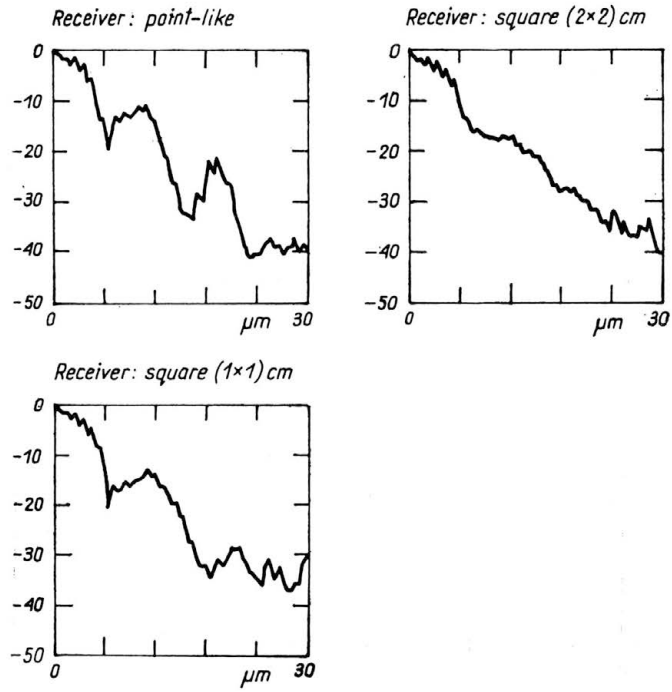

FIG. 8. Phase difference vs particle diameter for different receiver apertures at scattering angles 70°, ±4°. Beams angle — 4°, beams dimension — 300 μm, scattering angles {70°, 4°; 70°, −4°}.

In the third test intensity variations with particle diameter for different scattering angles and receiver apertures have been checked. The results are shown in Figs. 9 and 10, respectively, for (30°, 0) and (70°, 0) scattering angles. Also in this situation the oscillations, superimposed on the parabolic behaviour due to the particle cross-section, are averaged out with increasing dimension expecially for scattering angles equal to (30°, 0).

In the last test the visibility of the Doppler signal for different diameters, receivers dimensions and angle between the beams was examined. The visibility is the ratio

$$V = \frac{I_{max} - I_{min}}{I_{max} + I_{min}},$$

http://rcin.org.pl

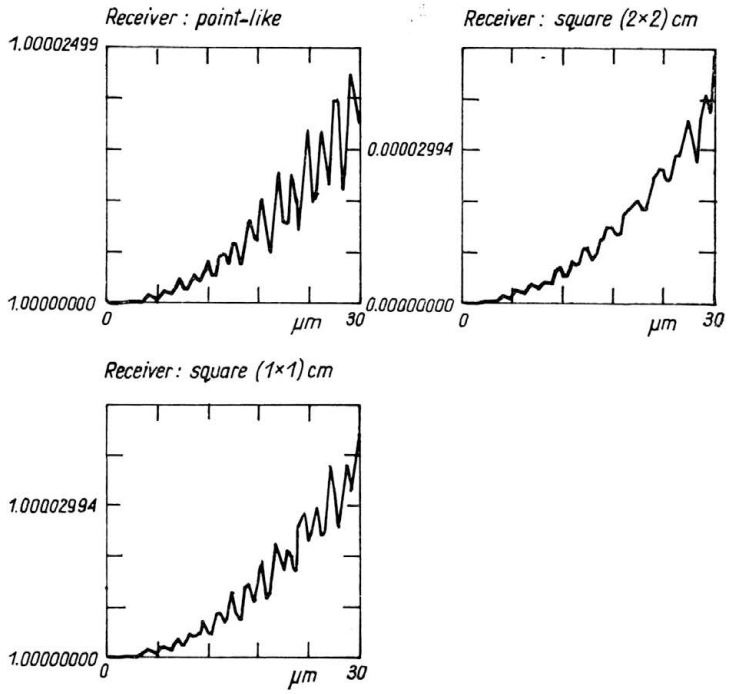

FIG. 9. Doppler signal intensity vs particle diameter for different revceiver apertures at a scattering angle of 30°. Beams angle — 4°, beams dimension — 300 μm, scattering angles — 30°, 0°.

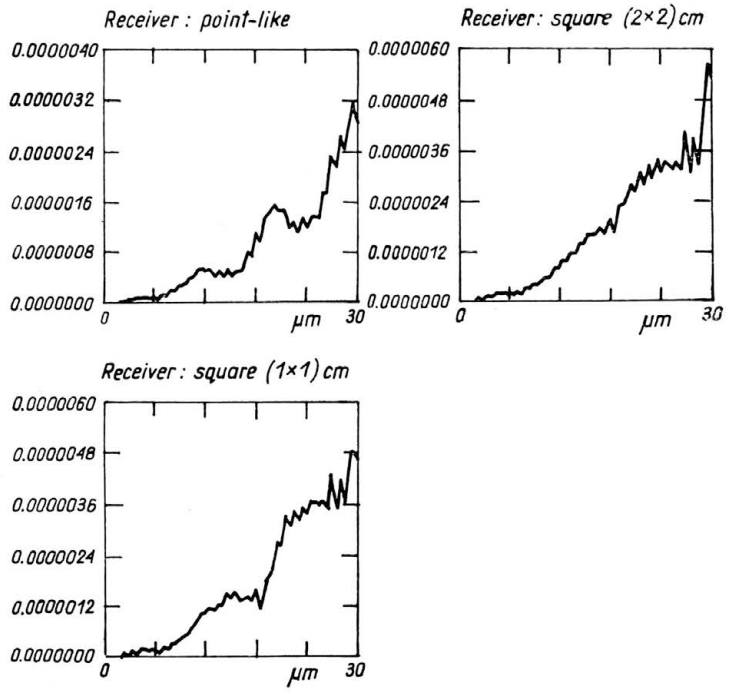

FIG. 10. Doppler signal intensity vs particle diameter for different receiver apertures at a scattering angle of 70°. Beams angle — 4°, beams dimension — 300 μm, scattering angles — 70°, 0°.

http://rcin.org.pl

where I_{max} and I_{min} indicate the intensity maximum and minimum. It is frequently used in particle sizing; however, it is not possible to obtain monotonous relationships between this quantity and the particle diameter in a large range of particle size.

In Fig. 11 visibility vs particle diameter has been plotted; it is possible to observe that in some particle diameter range a monotonic relationship exists. Changing the beams angle and the receiver dimensions, it is possible to modify this range but not to extend it too much. Trajectory effects do not seem to affect the results.

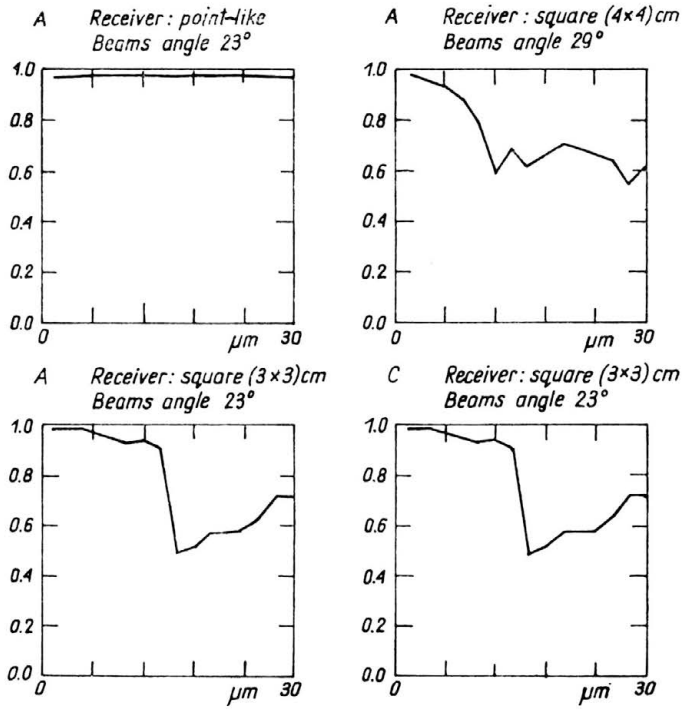

FIG. 11. Visibility vs particle diameter for different trajectories, receivers and angle between the two beams. Beams dimension — 300 μm, scattering angles — 0°, 40°, observed distance — 25 cm.

4. Conclusions

A three-dimensional Lorenz–Mie calculation program capable of simulating the diffused light from a spherical particle crossing the measuring volume produced by two intersecting Gaussian laser beams has been presented. The preliminary results give assurance of a reliable description of the light diffusion phenomena produced by the particle.

Three different quantities to evaluate the particle diameter have been considered: phase difference, absolute intensity and visibility. In all the situations the receiver aperture plays an important role; the oscillations due to spatial lobes are averaged out with increasing receiver dimensions. Furthermore the receiver position seems to be particularly delicate.

http://rcin.org.pl

For the linearity of the relation between the phase difference and the diameter of the particles it is advantageous to use a size measurement method based on phase difference detection; calibration problems, which are present in amplitude methods, are avoided. Monotonous trends cannot be found easily in visibility measurements; moreover, they hold only in a limited range of particle diameters.

Finally, the simulation of Doppler signals seems to indicate a criterion to derivate the trajectory of the particle in the measurement volume from the low frequency intensity component. This is one of the points that the authors are going to examine further.

Appendix A

In the three-axis coordinate system of Fig. 1, the unit vectors in the receiving, incident beam 1 and incident beam 2 directions are:

$$\begin{aligned}\mathbf{r} &= (\sin\theta\cos\Phi\mathbf{i}+\sin\theta\sin\Phi\mathbf{j}+\cos\theta\mathbf{k}),\\ \mathbf{i}_1 &= (-\sin\alpha\mathbf{j}+\cos\alpha\mathbf{k}),\\ \mathbf{i}_2 &= (\sin\alpha\mathbf{j}+\cos\alpha\mathbf{k}),\end{aligned}$$

where $\mathbf{i}$, $\mathbf{j}$, $\mathbf{k}$ are the x, y, z directions unit vectors, 2α is the angle between the beams and the angles θ, Φ are referred to the x, y, z-axis. The directions of the electric field components will be

$$\mathbf{E}_{\perp 1} = \frac{\mathbf{r}\times\mathbf{i}_1}{|\mathbf{r}\times\mathbf{i}_1|} = \frac{F_{\perp 1}\mathbf{i}+G_{\perp 1}\mathbf{j}+H_{\perp 1}\mathbf{k}}{L_{\perp 1}},$$

$$\mathbf{E}_{\perp 2} = \frac{\mathbf{r}\times\mathbf{i}_2}{|\mathbf{r}\times\mathbf{i}_2|} = \frac{F_{\perp 2}\mathbf{i}+G_{\perp 2}\mathbf{j}+H_{\perp 2}\mathbf{k}}{L_{\perp 2}},$$

$$\mathbf{E}_{\parallel 1} = \frac{(\mathbf{i}_1\cdot\mathbf{r})\mathbf{r}-\mathbf{i}_1}{|(\mathbf{i}_1\cdot\mathbf{r})\mathbf{r}-\mathbf{i}_1|} = \frac{F_{\parallel 1}\mathbf{i}+G_{\parallel 1}\mathbf{j}+H_{\parallel 1}\mathbf{k}}{L_{\parallel 1}},$$

$$\mathbf{E}_{\parallel 2} = \frac{(\mathbf{i}_2\cdot\mathbf{r})\mathbf{r}-\mathbf{i}_2}{|(\mathbf{i}_2\cdot\mathbf{r})\mathbf{r}-\mathbf{i}_2|} = \frac{F_{\parallel 2}\mathbf{i}+G_{\parallel 2}\mathbf{j}+H_{\parallel 2}\mathbf{k}}{L_{\parallel 2}}.$$

with

$$\begin{aligned}F_{\perp 1} &= \sin\alpha\cos\theta+\cos\alpha\sin\theta\sin\Phi,\\ G_{\perp 1} &= -\cos\alpha\sin\theta\cos\Phi,\\ H_{\perp 1} &= -\sin\alpha\sin\theta\cos\Phi,\\ L_{\perp 1} &= (F_{\perp 1}^2+G_{\perp 1}^2+H_{\perp 1}^2)^{1/2},\\ F_{\perp 2} &= -\sin\alpha\cos\theta+\cos\alpha\sin\theta\sin\Phi,\\ G_{\perp 2} &= -\cos\alpha\sin\theta\cos\Phi,\\ H_{\perp 2} &= \sin\alpha\sin\theta\cos\Phi,\\ L_{\perp 2} &= (F_{\perp 2}^2+G_{\perp 2}^2+H_{\perp 2}^2)^{1/2},\end{aligned}$$

$$\begin{aligned}F_{\parallel 1} &= -\sin\alpha\sin^2\theta\sin\Phi\cos\Phi+\cos\alpha\sin\theta\cos\Phi\cos\theta,\\ G_{\parallel 1} &= -\sin\alpha\sin^2\theta\sin^2\Phi+\cos\alpha\cos\theta\sin\theta\sin\Phi+\sin\alpha,\\ H_{\parallel 1} &= -\sin\alpha\sin\theta\sin\Phi\cos\theta+\cos\alpha\cos^2\theta-\cos\alpha,\end{aligned}$$

http://rcin.org.pl

$$
\begin{aligned}
L_{\|1} &= (F_{\|1}^2 + G_{\|1}^2 + H_{\|1}^2)^{1/2}, \\
F_{\|2} &= \sin\alpha \sin^2\theta \sin\Phi \cos\Phi + \cos\alpha \sin\theta \cos\Phi \cos\theta, \\
G_{\|2} &= \sin\alpha \sin^2\theta \sin^2\Phi + \cos\alpha \cos\theta \sin\theta \sin\Phi - \sin\alpha, \\
H_{\|2} &= \sin\alpha \sin\theta \sin\Phi \cos\theta + \cos\alpha \cos^2\theta - \cos\alpha, \\
L_{\|2} &= (F_{\|2}^2 + G_{\|2}^2 + H_{\|2}^2)^{1/2}
\end{aligned}
$$

and to obtain the complete expressions of the component along the x, y, z-axis, it is sufficient to multiply these quantities with Eq. (2.3) in the text. In this way it is possible to write the functions A, B, C, D, E defined in Eq. (2.5) as

$$
\begin{aligned}
A(\theta, \Phi, R) &= A_{\|1}^2/2 + A_{\perp 1}^2/2 + A_{\|2}^2/2 + A_{\perp 2}^2/2, \\
B(\theta, \Phi, R) &= \frac{A_{\|1} A_{\|2}}{L_{\|1} L_{\|2}} (F_{\|1} F_{\|2} + G_{\|1} G_{\|2} + H_{\|1} H_{\|2}), \\
C(\theta, \Phi, R) &= \frac{A_{\|1} A_{\perp 2}}{L_{\|1} L_{2\perp}} (F_{\|1} F_{\perp 2} + G_{\|1} G_{\perp 2} + H_{\|1} H_{\perp 2}), \\
D(\theta, \Phi, R) &= \frac{A_{\perp 1} A_{\|2}}{L_{\perp 1} L_{\|2}} (F_{\perp 1} F_{\|2} + G_{\perp 1} G_{\|2} + H_{\perp 1} H_{\|2}), \\
E(\theta, \Phi, R) &= \frac{A_{\perp 1} A_{\perp 2}}{L_{\perp 1} L_{\perp 2}} (F_{\perp 1} F_{\perp 2} + G_{\perp 1} G_{\perp 2} + H_{\perp 1} H_{\perp 2}),
\end{aligned}
$$

where the quantities A are calculated through recurrence relationships of Riccati–Besse and Legendre functions [11].

The terms containing $A_{\|1} A_{\perp 1}$ or $A_{\|2} A_{\perp 2}$ are vanishing identically: this fact reflects the absence of interference between the electric field components originated by the same beam.

Appendix B

From the angles θ, Φ in an x, y, z coordinate system, it is necessary to know the angles θ', θ'', Φ', Φ'' referred to the first and to the second beam; in this way it is possible to use the same calculation program of one beam for two beams only changing the angles

$$
\begin{aligned}
\Phi' &= \operatorname{arctg}\left(\operatorname{tg}\Phi + \frac{\operatorname{cotg}\theta \operatorname{tg}\alpha}{\cos\Phi}\right), \\
\Phi'' &= \operatorname{arctg}\left(\operatorname{tg}\Phi - \frac{\operatorname{cotg}\theta \operatorname{tg}\alpha}{\cos\Phi}\right), \\
\theta' &= \arccos\left[\frac{\cos\theta}{\cos\beta}\cos(\beta + \alpha)\right], \\
\theta'' &= \arccos\left[\frac{\cos\theta}{\cos\beta}\cos(\beta - \alpha)\right],
\end{aligned}
$$

with

$$
\beta = \operatorname{arctg}(\operatorname{tg}\theta \sin\Phi).
$$

http://rcin.org.pl

References

1. A. CENEDESE and F. CIOFFI, *Optical methods in two-phase flows: working principles*, Ing. Sanit., 1, 1987.
2. J. Y. SON and M. W. FARMER, *Intensity ratio method using LDV optical system*, Proc. of ICALEO, 1986.
3. M. TIMMERMANN, *Laser particle sizer velocimeter*, Proc. I Intern. Symp. on LDA, Lisbon 1982.
4. W. D. BACHALO and M. J. HOUSER, Optical Eng., **23**, 5, p. 583, 1984.
5. M. SAFFMAN, P. BUCHAVE and H. TANGER, *Simultaneous measurements of size, concentration and velocity of spherical particles by a Laser Doppler method*, Proc. II Symp. on LDA, Lisbon 1984.
6. G. MIE, Ann. der Phys., **25**, p. 373, 1908.
7. C. M. VAN DE HULST, *Light scattering by small particles*, Wiley, New York 1957.
8. M. BORN and E. WOLF, *Principles of optics*, Pergamon Press, Oxford 1970.
9. G. GREHAN, B. MAHEU and G. GOUSBET, *Localized approximation to the generalized Lorenz–Mie theory*, Proc. of ICALEO, 1986.
10. D. C. FERGUSON and I. G. CURRIE, *Theoretical evaluation of LDA techniques for two-phase flow measurements*, Paper presented at the III Intern. Symp. on LDA, Lisbon 1986.
11. F. DURST, A. MELLING and J. H. WHITELAW, *Principles and practice of LDA*, Academic Press, 1976.
12. C. BRIASCHI, *Analisi numerica ed applicazioni sperimentali dello scattering di Mie*, Tesi di Laurea, Milano 1979.
13. C. KERKER, *The scattering of light and other electro-magnetic radiation*, Academic Press, New York 1969.
14. F. DURST and B. ELIASSON, *Properties of LDA signals and their exploitation for particle size measurements*, Proc. of the LDA Symp., Copenhagen 1975.
15. S. A. M. AL CHALABI, Y. HARDALUPAS, A. R. JONES and A. M. K. P. TAYLOR, *Calculation of calibration curves for the phase Doppler technique: comparison between Mie theory and geometrical optics*, Proc. Symp. on Optical Particle Sizing, Rouen 1987.
16. W. J. GLANTSHNING and S. H. CHEN, Applied Optics, **20**, 2499, 1981.

DIPARTIMENTO DI MECCANICA E AERONAUTICA
and
DIPARTIMENTO DI IDRAULICA, TRANSPORTI E STRADE
UNIVERSITA' DI ROMA, „LA SAPIENZA" ROMA, ITALY.

Received October 28, 1987.

http://rcin.org.pl